Understanding the functionality of an array of invisibility cloaks

Mohamed Farhat,[1,*] Pai-Yen Chen,[2] Sébastien Guenneau,[3] Stefan Enoch,[3] Ross McPhedran,[4] Carsten Rockstuhl,[1] and Falk Lederer[1]

[1]*Institute of Condensed Matter Theory and Solid State Optics, Abbe Center of Photonics, Friedrich-Schiller-Universität Jena, D-07743 Jena, Germany*

[2]*Department of Electrical and Computer Engineering, The University of Texas at Austin, Austin, Texas 78712, USA*

[3]*Institut Fresnel, CNRS, Aix-Marseille Université, Campus Universitaire de Saint-Jérôme, F-13013 Marseille, France*

[4]*IPOS, School of Physics, University of Sydney, Sydney, New South Wales 2006, Australia*

(Received 16 June 2011; revised manuscript received 6 October 2011; published 1 December 2011)

This paper describes the operation and the interaction of cloaking devices when they are periodically arranged. The main focus is on analyzing the dispersion relation of structures, which should mimic that of the vacuum in the ideal scenario. We distinguish between two cloaking mechanisms: cloaks designed within the framework of transformation optics and cloaks designed on the basis of the scattering cancellation technique. The difference between the two approaches is that the first operates independently of the frequency by assuming nondispersive materials, whereas the latter is designed to operate for a single frequency. Our numerical simulations demonstrate that arrays made of such invisible dielectric obstacles act like a homogeneous medium with permittivity and permeability equal to those of the surrounding medium, except for a countable set of eigenfrequencies associated with Mie resonances for the former type of (transformation-based) cloak. For the latter type of (plasmonic) cloak, the marginal scattering response indicates the effectiveness of cloaking arrays of individual particles. Our spectral (Floquet-Bloch) approach to cloaking might be useful to implement realistic applications such as biomedical sensing, noninvasive probing, sensing networks, or multiobjective camouflaging.

DOI: 10.1103/PhysRevB.84.235105 PACS number(s): 42.25.Bs, 41.20.−q, 42.79.−e

I. INTRODUCTION

In recent years, conformal mapping and transformation optics paved the way to the implementation of numerous exotic applications, such as the ability to render arbitrary objects undetectable by exterior observers,[1,2] simulation of black holes,[3,4] gradient index lenses,[5] and hyperlenses.[6] Among all these effects, invisibility has attracted most of the attention of researchers since it is potentially the most counterintuitive and fascinating effect. Shortly after the publication of the seminal papers by Pendry *et al.*[1,7] and Leonhardt and Philbin,[2,8] where the concepts were introduced and the basic theoretical framework provided, an experimental study showed the possibility of hiding a 10-cm-long metallic cylinder from microwaves at the frequency of 8.5 GHz.[9] Generally, this mechanism requires simultaneously inhomogeneous and anisotropic material properties (tensors of permittivity ε and permeability μ), which are challenging to implement even with the most complex metamaterial at hand. Li and Pendry proposed to relax these constraints by introducing a new type of cloaking called *carpet cloaking*.[10] The carpet cloak makes any object placed above a ground plate appear as if it were a flat mirror by hiding it under a suitably designed metamaterial layer. It has the advantage that the required permittivity is isotropic and no longer singular. Shortly afterward, this concept was demonstrated to be powerful in designing invisibility devices; subsequent experiments were performed at both microwave[11] and infrared frequencies[12,13] and even recently in the optical domain.[14,15]

Parallel to these efforts, an alternative strategy was disclosed by Alù and Engheta in 2005.[16] It consists in the use of plasmonic materials (with near-zero or negative permittivity) to render dielectric or conducting objects nearly invisible. The proposed mechanism relies on a scattering cancellation technique, based on the negative local polarizability of a cover made of low-permittivity materials.[16–18] Further approaches to implement cloaking devices rely on an anomalous resonance of a cylindrical perfect lens to cloak a countable set of line sources,[19,20] homogenization of a quasiphotonic crystal of ellipsoids to mimic anisotropy,[21,22] or use of the waveguide approach.[23]

Most of these previous studies considered invisibility from the real space point of view, i.e., by analyzing the response of an isolated cloak to an external illumination (plane wave or Gaussian beam at fixed frequency). An alternative way to understand the functionality of the cloak, which we wish to elaborate on here, is to formulate it in terms of an eigenvalue problem as was done by Guenneau *et al.*, who analyzed cloaking of a periodic array of acoustic inclusions.[24] Light propagation in any medium is governed by the wave equation. Hence, light propagation from an initial plane located in front of the cloak toward a plane behind the cloak has to be indistinguishable from the propagation through the background material, i.e., the amplitude distribution and the phase advance have to be identical. Whereas the amplitude distribution has to be preserved between the planes, the absolute phase is allowed to vary, i.e., it will be the Bloch phase. What happens in between these planes is of minor importance and actually defines the modus operandi of the cloak. The primary question for defining a cloak therefore can be recast as a search for a desired material distribution between these two planes, in addition to a given obstacle, such that the eigenmodes and the eigenvalues will be exactly those of the homogeneous surroundings. The formulation of this eigenvalue problem is well established in certain fields of photonics, i.e., for photonic crystals, but also for metamaterials.[25] Consequently, one aim of this paper is to apply the methods from such fields to the

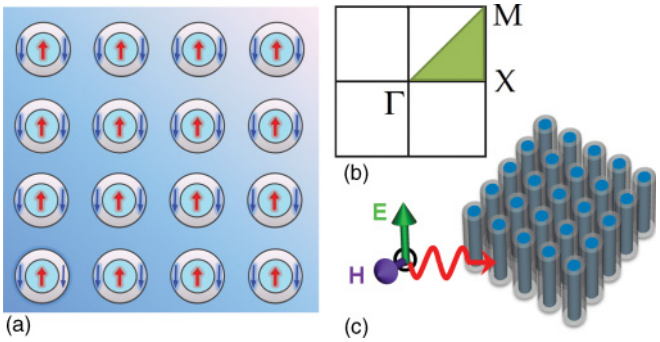

FIG. 1. (Color online) (a) Schematic of an array of cloaked dielectric cylinders in the two-dimensional (2D) geometry (for illustration we consider the example of plasmonic cloaks); this crystal is infinitely extended in all three directions. (b) First Brillouin zone ΓXM where $\Gamma = (0,0)$, $X = (\pi/a,0)$, and $M = (\pi/a,\pi/a)$, with a being the period of the array; dispersion diagrams will be computed along these directions. (c) Polarized plane wave incident on the structure composed of the cloaked cylinders.

present problem, which furthermore requires the cloaks to be periodically arranged in space. In fact, in some applications (such as sensing networks or multiobject camouflaging), one needs to cloak a periodic arrangement of particles, and thus the dispersion relations should be computed in order to verify the invisibility efficiency for the different Bloch modes (characterized by their frequencies and wave numbers).

Therefore, here we analyze cloaking devices and their spectral properties by relying on an analysis of the dispersion relation for periodically arranged cloaks. For this purpose, we address the problem of cloaking an array of dielectric or conducting obstacles, as depicted schematically in Fig. 1, by covering each of them with an invisibility shell (whose parameters are deduced from either the transformation optics approach or the plasmonic cancellation technique).

II. DISPERSION OF TRANSFORMATION-OPTICS-BASED CLOAKING DEVICES

A. Arrays of ideal cloaks and dispersionless modes

Recent mathematical results[26–29] show that, in the case of a single cylindrical cloak, there is a perfect correspondence between the waves in the (empty) virtual space and the waves in the physical space. For this to be proven mathematically, the axis of the cylinder should have zero capacity (in the sense of potential theory), which is obvious in the case of a single cloak. This also should be true for a 2D array of lines in a three-dimensional space or a 2D array of points in a two-dimensional space, and again a perfect correspondence between the waves in virtual and physical space, resulting in perfect cloaking, is expected to be observed. This is exactly what we wanted to test in this introductory section. The analysis of such a case using the dispersion relation serves moreover the purpose of verifying the accuracy of our numerical procedure. Light propagation through an array of ideal cloaks whose parameters are deduced from transformation optics[1] should not deviate from that of free space. With the confidence obtained concerning the predictive power of our methodology, the approach will be applied further below to the more relevant scenarios of imperfect cloaks, where the coherent interaction between adjacent entities sensitively affects the overall cloaking capabilities.

To calculate the dispersion relation, let us consider the case of TE-polarized electromagnetic waves $\mathbf{E} = E_3\mathbf{e}_3$ satisfying (without loss of generality)

$$\nabla \times [\mu^{-1}(x_1,x_2)\nabla \times \mathbf{E}(x_1,x_2)] - \varepsilon(x_1,x_2)k_0^2\mathbf{E}(x_1,x_2) = \mathbf{0}, \tag{1}$$

with $\varepsilon(x_1,x_2)$ and $\mu(x_1,x_2)$ the relative permittivity and permeability of the medium and $k_0 = \omega/c$ the free-space wave number. $\mathbf{E}(x_1,x_2)$ is a function of spatial variables and is of finite energy in $Y = [0;a]^2$ (square integrable and with a square integrable gradient) and such that

$$\mathbf{E}(x_1 + a, x_2 + a) = \mathbf{E}(x_1,x_2)e^{i(k_1+k_2)a}, \tag{2}$$

where the Bloch vector $\mathbf{k} = (k_1,k_2) \in Y^* = [0,\pi/a]^2$, and Y^* is the so-called first Brillouin zone (see Fig. 1). This square cell Y^* in reciprocal space can be further reduced to a square triangle ΓXM with vertices $\Gamma = (0,0)$, $X = (\pi/a,0)$, and $M = (\pi/a,\pi/a)$, as depicted in Fig. 1, if the inclusion within the cell Y in physical space exhibits a fourfold symmetry.

To enforce Floquet-Bloch conditions in Eq. (1), it suffices to link values of $\mathbf{E}$ on opposite sides of the basic cell Y.[31] The finite element formulation was implemented in the commercial package COMSOL multiphysics.[32]

The resolvent of the operator associated with the weak form of Eq. (1) is compact; hence for a given Bloch vector $\mathbf{k}$ the spectrum is a countable set of isolated eigenvalues tending to infinity. This spectrum can be ordered by increasing number $k_n(\mathbf{k})$ (with the integer n taking into account the multiplicity of a given eigenvalue $k_n = \omega_n/c$). More precisely, these eigenvalues can be numerically found using the Rayleigh quotient of (1) and invoking the Courant-Fischer min-max principle,[33] which says that, for all $n \geqslant 1$, one has

$$k_n^2(\mathbf{k}) = \min_{U_{n-1}\in H_{n-1}} \max_{0\neq\phi\in U_{n-1}^{\perp}} \frac{\int_Y \mu^{-1}|\nabla \times \mathbf{E}|^2\, dx_1dx_2}{\int_Y \varepsilon|\mathbf{E}|^2\, dx_1dx_2}, \tag{3}$$

where H_n is the set of subspaces of dimension n of the infinite-dimensional Hilbert space $H_\sharp(\mathbf{k},Y) = \{(\mathbf{E},\nabla \times \mathbf{E}) \in L^2(Y) \times [L^2(Y)]^2$, $\mathbf{E}$ satisfies (2)$\}$. The larger n, the finer is the approximation of $H_\sharp(\mathbf{k},Y)$ by H_n (density result). The numerical counterpart is nothing but the iterative Lanczos algorithm, which is well suited for large sparse matrices appearing in finite element methods.[31]

Figure 2 reveals the spectral behavior of the cloak whose parameters are given in Ref. 1 according to the Floquet-Bloch theory. Dispersion relations of ideal cloaks should be identical to those of free space; and there is a perfect correspondence between the waves in virtual and physical space, resulting in perfect cloaking as outlined above; we can see that this statement is verified for most of the spectral domain, whereas we can observe a marginal mismatch for some modes. This may be likely attributed to the requirements of an infinite permittivity and permeability[1] which are naturally not reached numerically or experimentally. The insets (a) and (b) of Fig. 2 show the snapshot of the electric field corresponding to the first two eigenmodes at $X = (\pi/a,0)$ and the streamlines of the field, which demonstrate clearly the behavior predicted by the

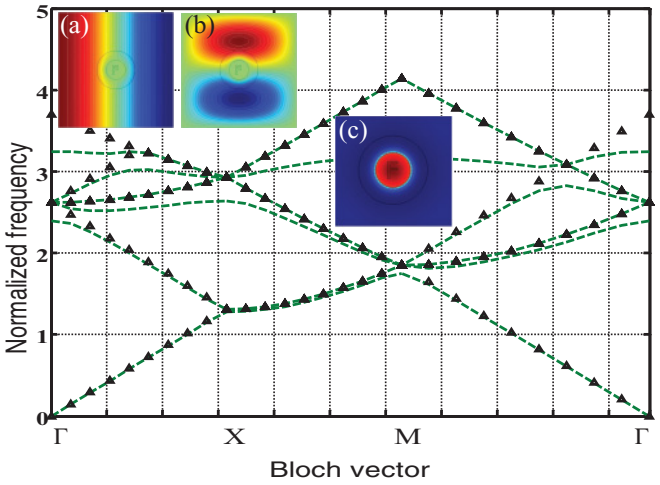

FIG. 2. (Color online) Dispersion diagram for a doubly periodic array (pitch a) of cloaked electromagnetic obstacles (in dashed line) with a shell of inner and outer radii of $0.2a$ and $0.4a$, respectively, in the first Brillouin zone ΓXM where $\Gamma = (0,0)$, $X = (\pi/a,0)$, and $M = (\pi/a,\pi/a)$ (schematic representing the unit cell of the array is drawn in the inset (a) of the figure). The triangles represent the dispersion in vacuum and are given for comparison as well as to test the efficiency of the cloak. In the insets (a) and (b), the first two eigenmodes of the structure are depicted. We show here a snapshot of the electric field in the unit cell at point X, where $X = (\pi/a,0)$, and the streamlines that seem to be curved when passing through the cloaking device as predicted by the geometrical transformations. The inset (c) gives the fourth mode at point M, $M = (\pi/a,\pi/a)$, which is a localized one corresponding to the resonance of a cavity of radius R_1 [a Mie resonance called an almost-trapped eigenstate in the context of quantum cloaks by Greenleaf *et al.* (Ref. 30)]. It is important to note that we found a discrete set of such dispersionless modes at higher frequencies, all of which were associated with Mie resonances of the cavity (monopole, dipole, quadrupole, and so forth).

coordinate transform paradigm, i.e., the field lines seem to be curved when passing through the cloak region and propagate as if there were no obstacle in their way. We mention that the only large deviation concerns the appearance of a fourth-order mode which does not have a counterpart in the vacuum dispersion curve. It is a localized mode of the inner cavity of radius R_1 reminiscent of the quasitrapped modes discovered by Greenleaf *et al.*[30] The inset (c) of Fig. 2 shows that the energy of the field is entirely concentrated inside this cavity. We note that this mode is dispersionless as it does not interact with its surroundings, i.e., it is entirely confined within the inner region of the cloak.

Thus it is obvious that, except for the dispersionless mode which cannot interact with the exterior, our numerical procedure shows an excellent agreement between the dispersion of the array of cloaks and dispersion in vacuum. This allows us to move to the core of our work, which consists in analyzing realistic cloaks based on either transformation optics or the plasmonic cancellation technique.

B. Spectral properties of multilayered cloaks

We now turn to the analysis of a practical structure, based on transformation optics; the structure consists of concentric multilayers behaving as an anisotropic medium in the homogenization limit, as proposed first in Ref. 34. Electromagnetic layered systems with two alternating isotropic materials (A and B) can produce a transversely isotropic system whose effective permeability μ is a tensor, as can be seen from Fig. 3(a). Reduced forms of permittivity are necessary in order to manufacture realistic cloaking devices.[9] This mechanism is imperfect by definition, since we loosen the requirements on ε and μ by combining these two requirements into one through the refractive index. Then our proposed structure consists of alternating concentric layers A and B with the same thickness d. Layers of kind A have their permeability slowly varying whereas layers of kind B have rapidly varying permeability. This means that the arithmetic average μ_ϕ is almost constant, and the geometric average μ_r has the radial dependence given by Eq. (4). The size of these layers is much smaller than the incident wavelength λ, and in this limit has the following effective permittivity and permeability tensors:

$$\mu_r = \frac{2\mu_A\mu_B}{\mu_A+\mu_B}, \quad \mu_\phi = \frac{\mu_A+\mu_B}{2}, \quad \varepsilon_3 = \frac{\varepsilon_A+\varepsilon_B}{2}. \tag{4}$$

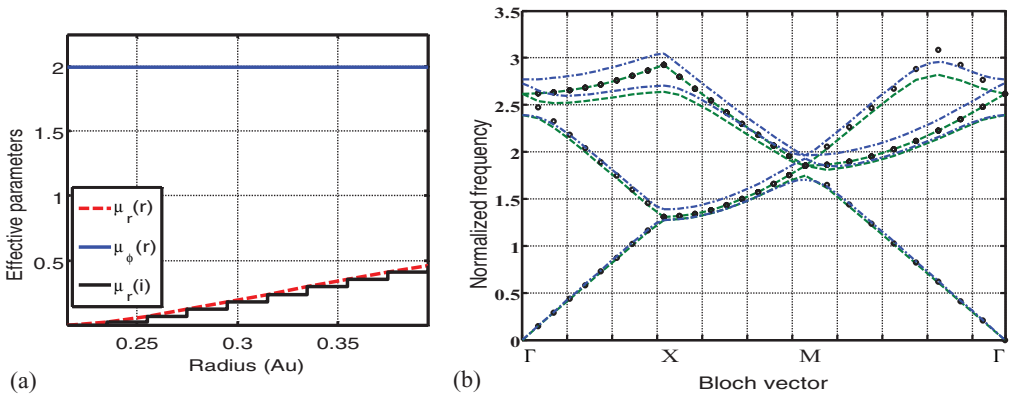

FIG. 3. (Color online) (a) Radial dependence of reduced electromagnetic parameters μ_r and μ_ϕ obtained from the geometric transform in blue (light gray) and red (dotted line) and corresponding staircase approximation $\mu_r(i)$, $i = 1,\ldots,20$, for the layered cloak consisting of ten cells of alternating isotropic homogeneous layers (black solid line). The relative permittivity ε_3 is constant and equal to 0.5. (b) The same as Fig. 2 but for a cloak made of the multilayered system described by Eq. (4). The dispersion of ideal cloak (dashed line), vacuum (dots) are compared to those of the cloak of Fig. 3(b). (dotted-dashed line).

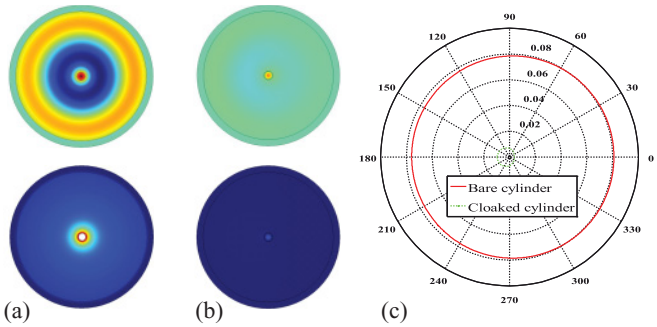

FIG. 4. (Color online) Scattered electric energy from the obstacle in vacuum (a) and when the cloak is turned on (b). The upper panels of (a) and (b) show the the electric field component E_3, while the lower ones represent the total energy. (c) Radar cross sections of the bare (solid line) and the cloaked cylinder (dashed line).

Using ten layers from each material, we can build a broadband cloak for electromagnetic waves. In Fig. 3(a) we show the theoretical permeability and its staircase approximation when we use $N = 10$ layers from each material A and B. Figure 3(b) shows the calculated dispersion diagram for such a cloak and compares it to the one for free space. From this figure, we can see that the agreement between the two scenarios is excellent, especially for the first two Bloch modes, where the homogenization limit is respected ($\lambda \gg d$). One should also mention that an increase in the number of layers will improve the performance of the cloak.

III. DISPERSION OF PLASMONIC CLOAKS

A. Introduction to scattering cancellation technique

Another area of active research activity in cloaking is that of plasmonic shells. In a way similar to the question addressed in the previous section, it seems legitimate to wonder whether cloaking by plasmonic resonances among a system of particles is a cooperation or competition, as first noted by McPhedran *et al.*,[35] and thus what happens for an array of such cloaks. Here again, we shall see that the answer is not trivial.

By analyzing the form of the scattered field from a spherical (dielectric or metallic) object, Alù and Engheta showed that, in the quasistatic limit, addition of a plasmonic coat with near- or less than zero effective permittivity permits a drastic reduction in the scattering cross section.[16,17] To understand this, let us consider the illumination of the structure by a plane wave propagating in the x direction, with an electric field polarized along the $\mathbf{e}_3$ axis. In the cylindrical case, the scattered field can be expanded in terms of Hankel functions as

$$E_3^{\mathrm{sca}}(r) = \sum_{m=0}^{m=+\infty} (2 - \delta_{m,0}) i^{\mathrm{m}} c_m H_m^{(1)}(k_0 r) \cos(m\phi), \qquad (5)$$

where δ_m,0 is the Kronecker symbol, i is the pure imaginary number, ϕ is the azimuthal angle, c_m is the scattering coefficient, and k_0 is the wave number. The corresponding normalized total scattering cross section is given by[36]

$$C_{\mathrm{sca}} = \frac{4}{k_0} \sum_{m=0}^{m=+\infty} (2 - \delta_{m,0}) |c_m|^2, \qquad (6)$$

where $c_m = -U_m/(U_m + iV_m)$ are the scattering coefficients and U_m and V_m are determinants of 4×4 matrices (see Ref. 16 for a complete derivation). In the quasistatic limit ($\lambda/a_s \gg 1$), the expression of the nth scattering order simplifies, and it can be shown that it scales as order $(k_0 a_s)^n$. This means, that C_{sca} is dominated by the zeroth order, which corresponds to the dipolar approximation. The expression for c_0 is

$$c_0 \approx \frac{-i\pi k_0^2}{4} \left[(\varepsilon_s - \varepsilon_c) a_s^2 - (\varepsilon_s - 1) a_c^2 \right]. \qquad (7)$$

It is clear from Eq. (7) that an analytical result can be provided that links the core radius a_c and its permittivity ε_c to the required shell radius a_s and permittivity $\varepsilon_s(\omega)$ in order to suppress the entire scattered signal. It turns out that[16]

$$\gamma^2 = \frac{\varepsilon_s - 1}{\varepsilon_s - \varepsilon_c}, \qquad (8)$$

with $\gamma = a_c/a_s$ (a shell, in simple words, that possesses the properties specified by this equation acts as an antireflection

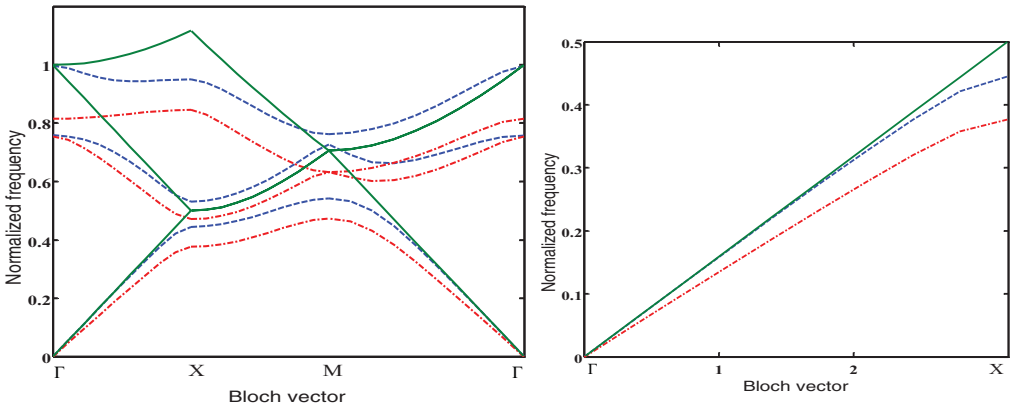

FIG. 5. (Color online) (a) Dispersion of a plasmonic cloak in blue (dashed) line compared to vacuum in solid line and the bare obstacle in dashed-dotted line. Simple case where the permittivity of the medium is taken to be constant, $\varepsilon_{\mathrm{ideal}} = -3.5454 + \delta i$, where δ is a small imaginary part, to mimic loss. (b) Zoom on the direction ΓX, where the scattering is governed by the dipole term, and where we expect the structure to be invisible: the dispersion curves of the core-shell system almost coincide with those of vacuum, and the agreement is better in the zero-frequency limit (quasistatic case) within the homogenization regime as indicated by the dotted ellipses in (a).

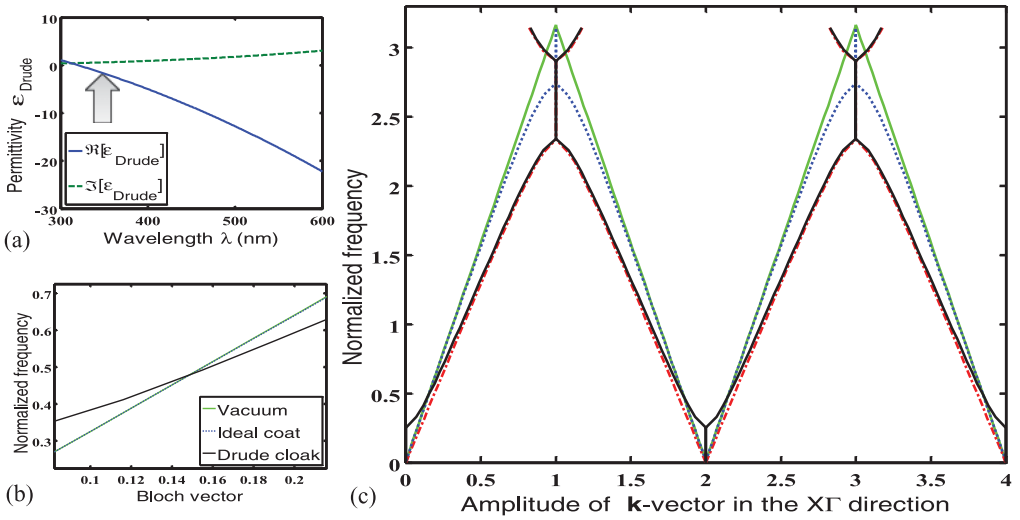

FIG. 6. (Color online) Dispersion of a plasmonic cloak. (a) The permittivity of the shell follows the well-known Drude model (dashed line gives the dispersion of the ideal cloak, green (light gray) one stands for vacuum, while dashed-dotted line corresponds to the bare obstacle and black (dark gray) gives the dispersion of the Drude's cloak). (b) Zoom on the region where $\mathrm{Re}(\varepsilon) = \varepsilon_{\mathrm{ideal}} = -3.5454$ and where the Drude shell is supposed to cloak perfectly the dielectric obstacle. This can be observed, since the two curves have an intersection point at $\omega/\omega_p \approx 0.47$ [as indicated by the arrow in (a)]. (c) Complete dispersion diagram showing the normalized frequency versus the modulus of the Bloch vector in the $X\Gamma$ direction for the bare obstacle (red), the vacuum (green), and the obstacle with the ideal shell (blue) and with the Drude shell (black).

coating for the core). Figure 4 shows the results of the numerical simulations of such a cloak and confirms this mechanism in the quasistatic limit. The shell can be made from a natural material or from a metamaterial itself to provide specific values at a desired target frequency.[37]

B. Spectral analysis of plasmonic cloaks

Let us now consider first the dispersion of a cloak consisting of a single layer of plasmonic material given by Eq. (8). In Fig. 5 the material dispersion of the plasmonic layer is not taken into account. It is clear from this figure that the Bloch modes of the cloak coincide with those of vacuum at relatively low frequencies [for the regions ΓX and $M\Gamma$ and around the Γ point as can be seen from Fig. 5 (b)]. For higher modes and thus frequencies (smaller wavelengths), the modes of the cloaked obstacle are still closer to those of vacuum than those of the bare obstacle, but a discrepancy between the first modes should be noticed. This can be explained by the fact that the quasistatic limit ceases to be valid, and the dipole contribution to the scattering cross section is no longer dominant. Then, the permittivity of Eq. (8) does not completely cancel the scattered field as it does in the long-wavelength limit.

Now we proceed with the more realistic case by taking into account the material dispersion relying on the Drude model $\varepsilon = \varepsilon_\infty - \omega_p^2/(\omega^2 - i\gamma\omega)$, where ω_p is the plasma frequency of the metal (2175 THz for silver), γ is the damping constant (4.35 THz for silver), and $\varepsilon_\infty = 1$. The problem in computing dispersion curves with frequency-dependent permittivity is that the eigenvalue problem is now nonlinear and requires another formulation for computing the eigenmodes conveniently. Davanço *et al.* proposed a different formulation for this class of problems, consisting of using the complex modulus of the Bloch vector as the eigenvalue for both a fixed frequency ω and the direction of the **k** vector.[38] Figure 6 displays the band structure of a square-lattice plasmonic crystal as function of the real part of the Bloch vector for vacuum, the bare obstacle, and the cloaked structure. As can be seen from Figs. 6(a) and 6(b), cloaking is matched when the value of $\varepsilon_{\mathrm{Drude}}$ satisfies Eq. (8), in agreement with the plasmonic cloaking predictions. To enhance the bandwidth of operation, many layers of different metals (with different plasma frequencies $\omega_{p,i}$) are needed, as shown in Ref. 17.

IV. CONCLUSION

The invisibility of arrays of coated particles was numerically studied using methods of both transformation optics and the plasmonic scattering cancellation technique. The dispersion curves of Bloch modes associated with these structures show an invisibility effect for the entire spectrum, *except for a discrete set of eigenfrequencies associated with Mie resonances of the invisibility region*, when transformation optics is used. In contrast, scattering reduction could be achieved with plasmonic coatings only in a narrow band. Our results show that it is possible to cloak an array of dielectric particles for a large range of frequencies independently of their shapes or the period of the photonic crystal which they constitute. Unlike most of the previous studies, which focused only on the scattering properties of cloaks, here we presented another point of view by analyzing their spectral response in terms of the dispersion relation, which unveiled the role played by quasitrapped modes in the collective response of an array of coated particles. This study could be of use for many devices, such as low-interference communication (for example, when one has an array of cloaked antennas), sensing, and detection. We are confident this will be beneficial for a variety of real-world applications, including biomedical sensing, noninvasive probing, sensing networks, multiobjective camouflaging, communications, and information processes.

We finally believe that this provides an additional perspective for studying these structures.

ACKNOWLEDGMENTS

Financial support by the Federal Ministry of Education and Research PhoNa, from the State of Thuringia within the ProExcellence program MeMa, as well as from the European Union FP7 Project NANOGOLD is acknowledged. R.C.M. acknowledges support from Australian Research Council Discovery Grants and Centre of Excellence Schemes. The authors want also to acknowledge insightful comments from the reviewer, which greatly helped to improve the quality of the paper.

*mohamed.farhat@uni-jena.de

[1] J. B. Pendry, D. Schurig, and D. R. Smith, Science **312**, 1780 (2006).
[2] U. Leonhardt, Science **312**, 1777 (2006).
[3] A. G. Dentcho, S. Zhang, and X. Zhang, Nat. Phys. **5**, 687 (2009).
[4] E. E. Narimanov and A. V. Kildishev, Appl. Phys. Lett. **95**, 041106 (2009).
[5] D. R. Smith, J. J. Mock, A. F. Starr, and D. Schurig, Phys. Rev. E **71**, 036609 (2005).
[6] Z. Liu, H. Lee, Y. Xiong, C. Sun, and X. Zhang, Science **315**, 1686 (2007).
[7] D. Schurig, J. B. Pendry, and D. R. Smith, Opt. Express **14**, 9794 (2006).
[8] U. Leonhardt and T. G. Philbin, New J. Phys. **8**, 247 (2006).
[9] D. Schurig, J. J. Mock, J. B. Justice, S. A. Cummer, J. B. Pendry, A. F. Starr, and D. R. Smith, Science **314**, 977 (2006).
[10] J. Li and J. B. Pendry, Phys. Rev. Lett. **101**, 203901 (2008).
[11] R. Liu, C. Ji, J. J. Mock, J. Y. Chin, T. J. Cui, and D. R. Smith, Science **323**, 366 (2009).
[12] J. Valentine, J. Li, T. Zentgraf, G. Bartal, and X. Zhang, Nat. Mater. **8**, 568 (2009).
[13] L. H. Gabrielli, J. Cardenas, C. B. Poitras, and M. Lipson, Nat. Photonics **3**, 461 (2009).
[14] T. Ergin, N. Stenger, J. B. Pendry, P. Brenner, and M. Wegener, Science **328**, 337 (2010).
[15] J. Fischer, T. Ergin, and M. Wegener, Opt. Lett. **36**, 2059 (2011).
[16] A. Alù and N. Engheta, Phys. Rev. E **72**, 016623 (2005).
[17] A. Alù and N. Engheta, Phys. Rev. Lett. **100**, 113901 (2008).
[18] B. Edwards, A. Alù, M. G. Silveirinha, and N. Engheta, Phys. Rev. Lett. **103**, 153901 (2009).
[19] N. A. Nicorovici, R. C. McPhedran, and G. W. Milton, Phys. Rev. B **49**, 8479 (1994).
[20] N. A. P. Nicorovici, G. W. Milton, R. C. McPhedran, and L. C. Botten, Opt. Express **15**, 6314 (2007).
[21] W. Cai, U. K. Chettiar, A. V. Kildiev, and V. M. Shalaev, Nat. Photonics **1**, 224 (2007).
[22] M. Farhat, S. Guenneau, A. B. Movchan, and S. Enoch, Opt. Express **16**, 5656 (2008).
[23] I. I. Smolyaninov, V. N. Smolyaninova, A. V. Kildishev, and V. M. Shalaev, Phys. Rev. Lett. **102**, 213901 (2009).
[24] S. Guenneau, A. B. Movchan, F. Zolla, N. V. Movchan, and A. Nicolet, J. Comput. Appl. Math. **234**, 1962 (2010).
[25] J. Petschulat, C. Menzel, A. Chipouline, C. Rockstuhl, A. Tünnermann, F. Lederer, and T. Pertsch, Phys. Rev. A **78**, 043811 (2008).
[26] A. Greenleaf, Y. Kurylev, M. Lassas, and G. Uhlmann, Commun. Math. Phys. **275**, 749 (2007).
[27] R. Weder, J. Phys. A **41**, 415401 (2008).
[28] R. V. Kohn, D. Onofrei, M. S. Vogelius, and M. I. Weinstein, Commun. Pure Appl. Math. **63**, 973 (2010); **63**, 1525 (2010).
[29] H. Nguyen, Commun. Pure Appl. Math. **63**, 1505 (2010).
[30] A. Greenleaf, Y. Kurylev, M. Lassas, and G. Uhlmann, Phys. Rev. Lett. **101**, 220404 (2008).
[31] A. Nicolet, S. Guenneau, C. Geuzaine, and F. Zolla, J. Comput. Appl. Math. **168**, 321 (2004).
[32] [www.comsol.com].
[33] C. Conca, J. Planchard, and M. Vaninnathan, *Fluids and Periodic Structures,* RAM: Research in Applied Mathematics (Wiley, New York, 1995).
[34] Y. Huang, Y. Feng, and T. Jiang, Opt. Express **15**, 11133 (2007).
[35] R. C. McPhedran, N. A. Nicorovici, L. C. Botten, and G. W. Milton, C. R. Phys. **10**, 391 (2009).
[36] J. D. Jackson, *Classical Electrodynamics*, 3rd ed. (Wiley, New York, 1999).
[37] S. Mühlig, M. Farhat, C. Rockstuhl, and F. Lederer, Phys. Rev. B **83**, 195116 (2011).
[38] M. Davanço, Y. Urzhumov, and G. Shvets, Opt. Express **15**, 9681 (2007).